

Cobalt complexes of Biginelli derivatives as fluorescent probes for selective estimation and degradation of organophosphates in aqueous medium

Gaganpreet Kaur,^a Amanpreet Singh,^b Ajnesh Singh,^c Navneet Kaur,^{d*} Narinder Singh^{b*}

^aCentre for Nanoscience & Nanotechnology, Panjab University, Chandigarh, 160014, India.

^bDepartment of Chemistry, Indian Institute of Technology Ropar (IIT Ropar), Rupnagar, Panjab, 140001, India. Email: nsingh@iitrpr.ac.in

^cDepartment of Applied Sciences and Humanities, Jawaharlal Nehru Government Engineering College, Sundernagar, Mandi (H.P.), 175018, India.

^dDepartment of Chemistry, Panjab University Chandigarh, 160014, India. Email: navneetkaur@pu.ac.in

Table of Contents

Figure S1. ¹H NMR spectrum of ligand L1 in CDCl₃.

Figure S2. ¹³C NMR of ligand L1 in CDCl₃.

Figure S3. ¹H NMR spectrum of ligand L2 in DMSO.

Figure S4. ¹³C NMR of ligand L2 in DMSO.

Figure S5. Mass spectrum of ligand L1.

Figure S6. Mass spectrum of ligand L2.

Figure S7. FTIR spectrum of ligand L1 (below) and its metal complex (top).

Figure S8. FTIR spectrum of ligand L2 (below) and its metal complex (top).

Figure S9. (A) Fluorescence spectra of ligand L1 in DMSO (10 μM) and its corresponding metal complex L1.Co (II). (B) Fluorescence spectra of ligand L2 in DMSO (10 μM) and its corresponding metal complex L2.Co (II).

Figure S10. Packing diagram of complex L 1.Co (II) shown down c axis (hydrogen bonding is shown by dotted pink lines).

Figure S11. Packing diagram of complex L2.Co (II) shown down c axis.

Figure S12. TGA graph of L1.Co (II) and L2.Co (II) complexes between the temperature range from 20 to 800 °C with the heating rate of 10 °C/minute.

Figure S13. (A) UV- Vis absorption spectra of metal complex L1.Co (II) in DMSO and in aqueous medium. (B) UV- Vis absorption spectra of metal complex L2.Co (II) in DMSO and in aqueous medium.

Figure S14. Non-linear regression graph between the emission intensity and concentration of Malathion added.

Figure S15. Non-linear regression graph between the emission intensity and concentration of Azamethiphos added.

Figure S16. (A) UV-Vis absorption profile of metal complex L1.Co (II) in water upon addition of different organophosphates. (B) Titration of L1.Co (II) with increasing concentration of Malathion.

Figure S17. (A) UV- Vis absorption profile of metal complex L2.Co (II) in water upon addition of different organophosphates. (B) Titration of L2.Co (II) with increasing concentration of Azamethiphos.

Figure S18. (A) Competitive binding experiment of L1.Co (II) complex containing 30 μM of Malathion and 60 μM of other OPs under study.

Figure S19. (A) Competitive binding experiment of L2.Co (II) complex containing 30 μM of Azamethiphos and 60 μM of other OPs under study.

Figure S20. Mass spectra showing the degradation products of Malathion.

Figure S21. Change in ^{31}P -NMR signal of Malathion upon degradation with time.

Figure S22. Mass spectra showing the degradation products of Azamethiphos.

Figure S23. Change in ^{31}P -NMR signal of Azamethiphos upon degradation with time.

Figure S24. Kinetic plots showing the reaction of Malathion with L1.Co (II) in buffer solution. Initial half-life ($t_{1/2}$) was calculated by plotting \ln of the conversion versus time; the slope (k) is related to the half-life by $t_{1/2} = \ln 2/k$.

Figure S25. Kinetic plots showing the reaction of Azamethiphos with L2.Co (II) in buffer solution. Initial half-life ($t_{1/2}$) was calculated by plotting \ln of the conversion versus time; the slope (k) is related to the half-life by $t_{1/2} = \ln 2/k$.

Table S1. Crystal data and refinement parameters of L1.Co (II).

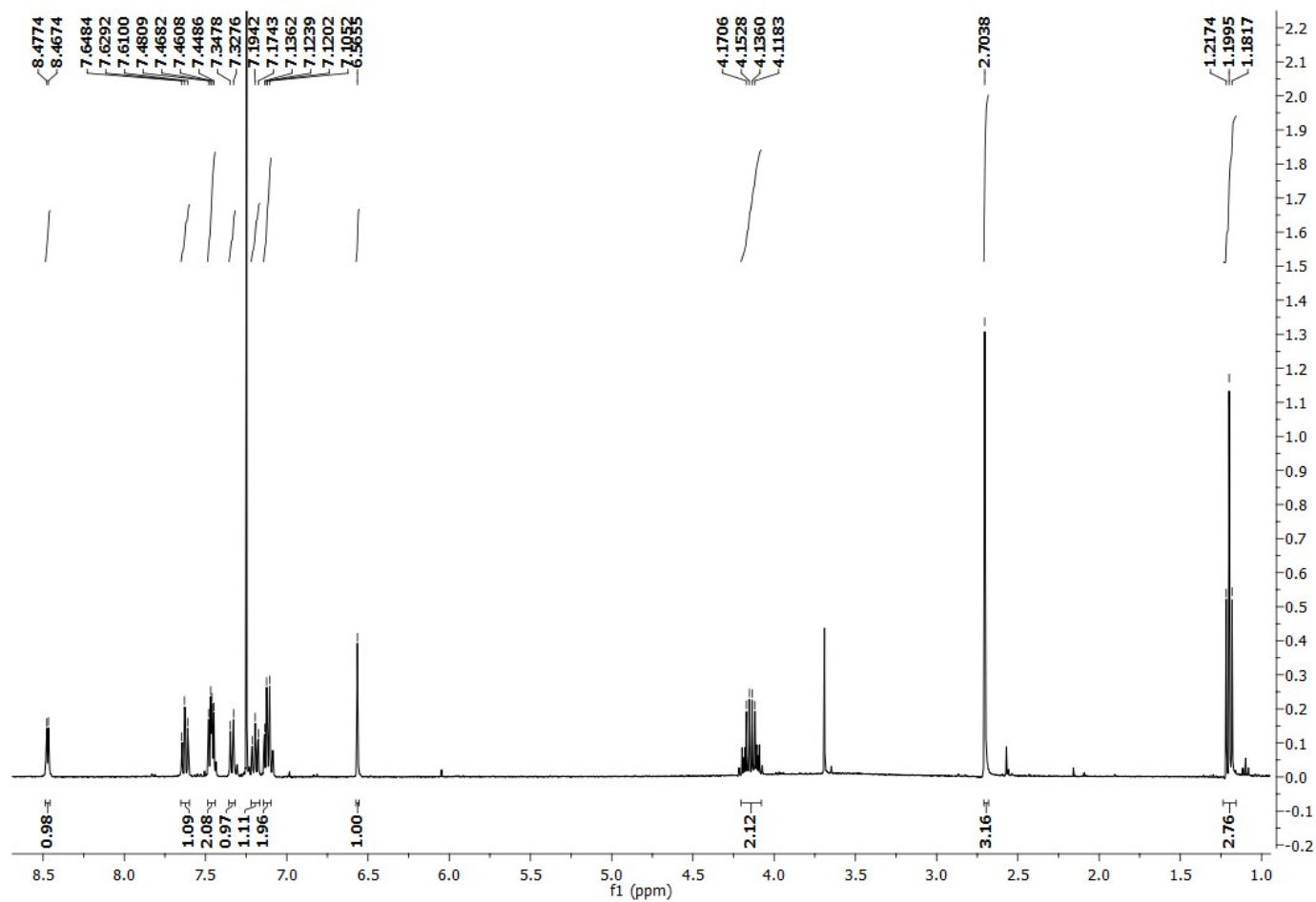
Table S2. Selected bond lengths and angles (\AA , $^\circ$) for complex L1.Co (II).

Table S3. Hydrogen bonding parameters (\AA , $^\circ$) of L1.Co (II)

Table S4. Crystal data and refinement parameters of L2.Co (II).

Table S5. Selected bond lengths and angles (Å,°) for complex L2.Co (II).

Table S6. Hydrogen bonding parameters (Å, °) of L2.Co (II)



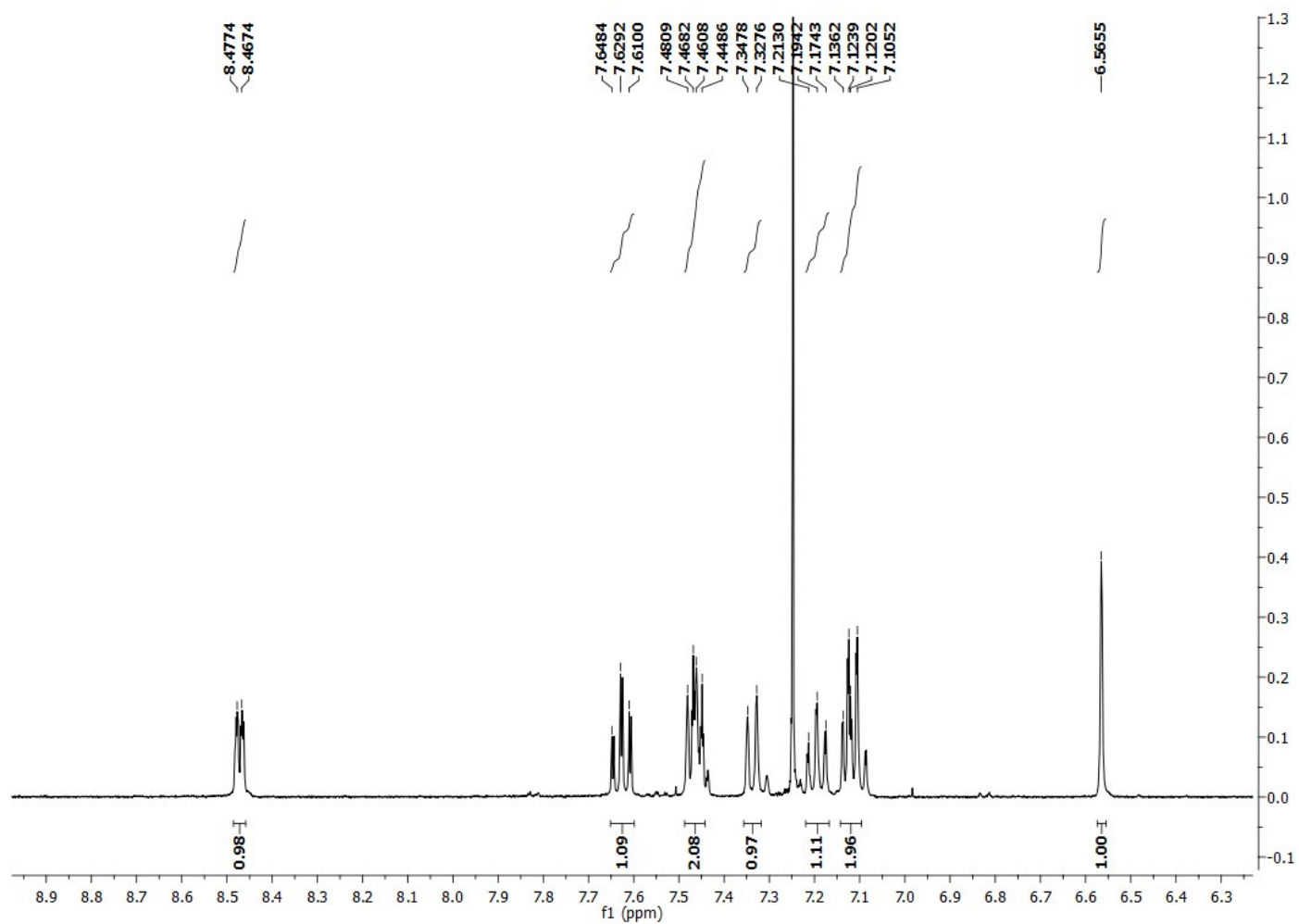


Figure S1. ^1H NMR spectrum of ligand L1 in CDCl_3 and its expansion.

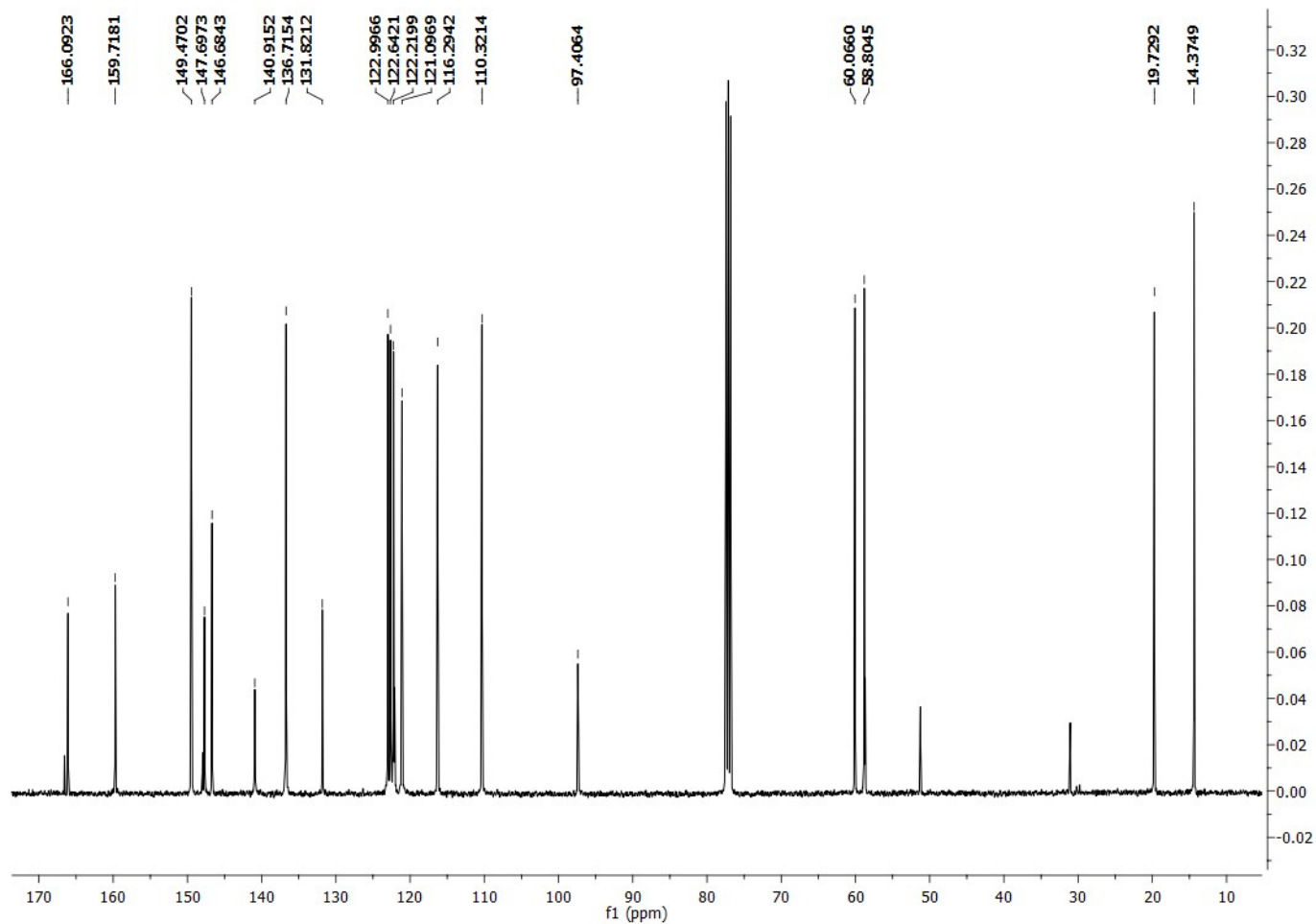
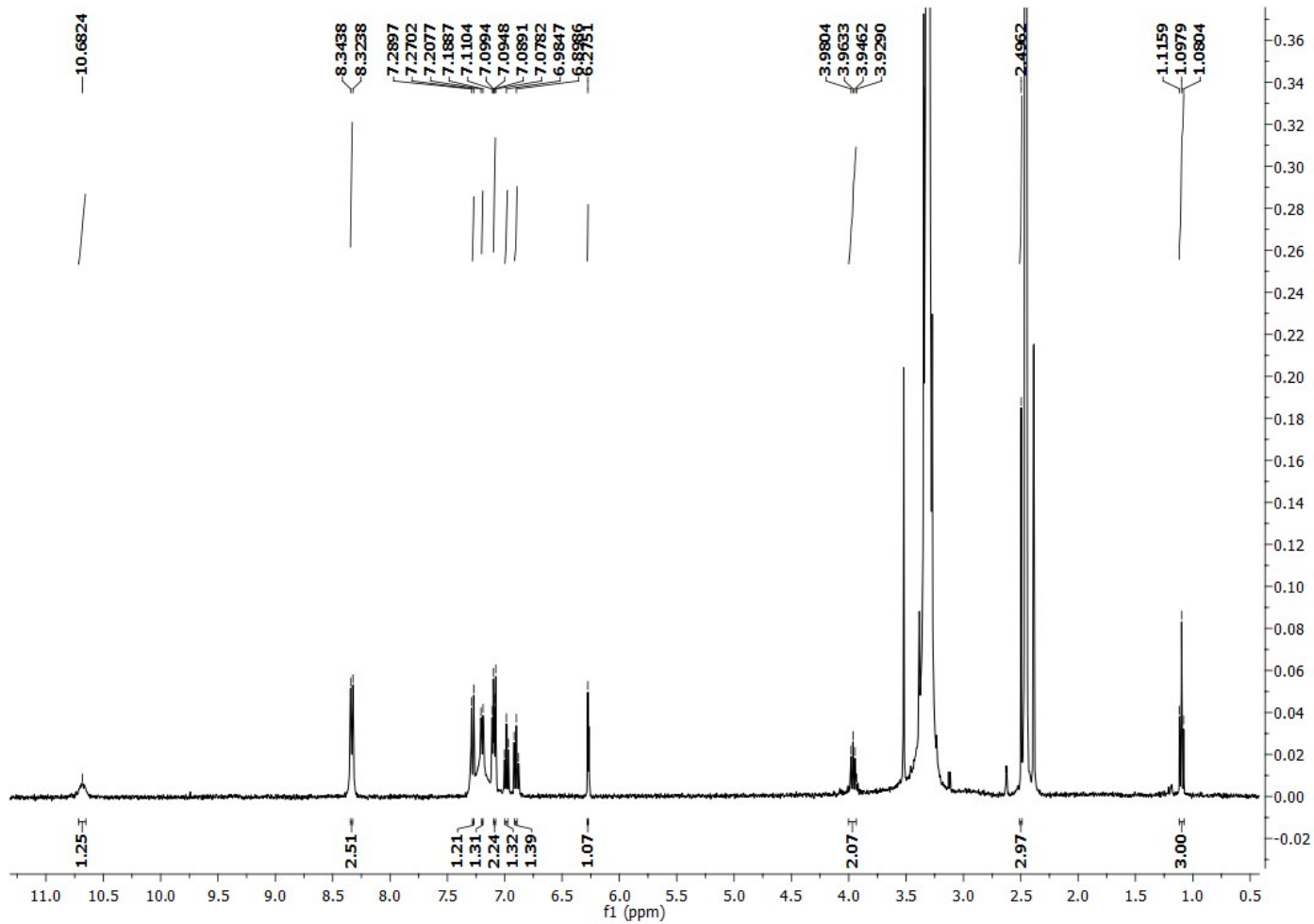


Figure S2. ^{13}C NMR of ligand L1 in CDCl_3 .



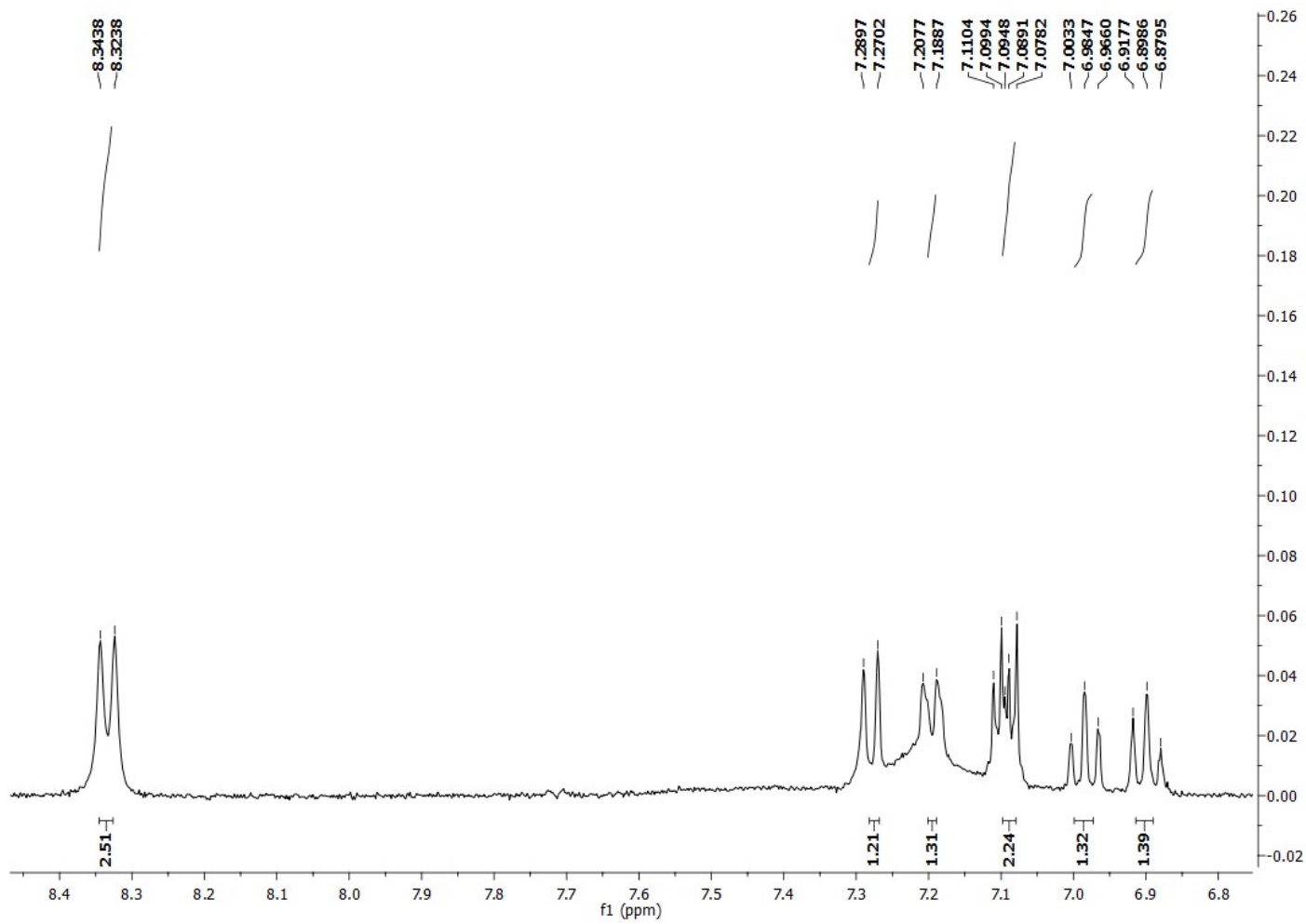


Figure S3. ^1H NMR spectrum of ligand **L2** in DMSO and its expansion.

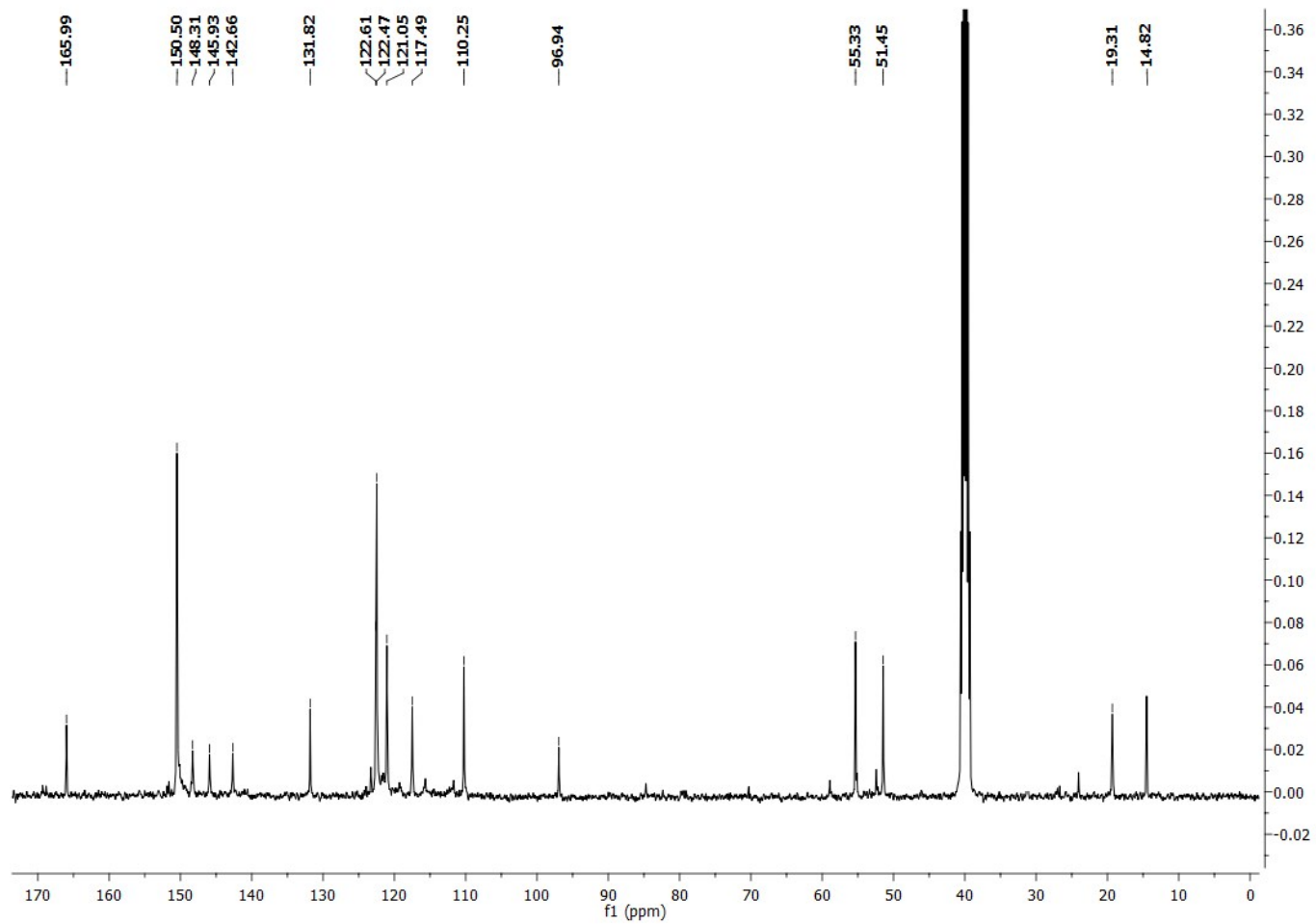


Figure S4. ^{13}C NMR of ligand L2 in DMSO.

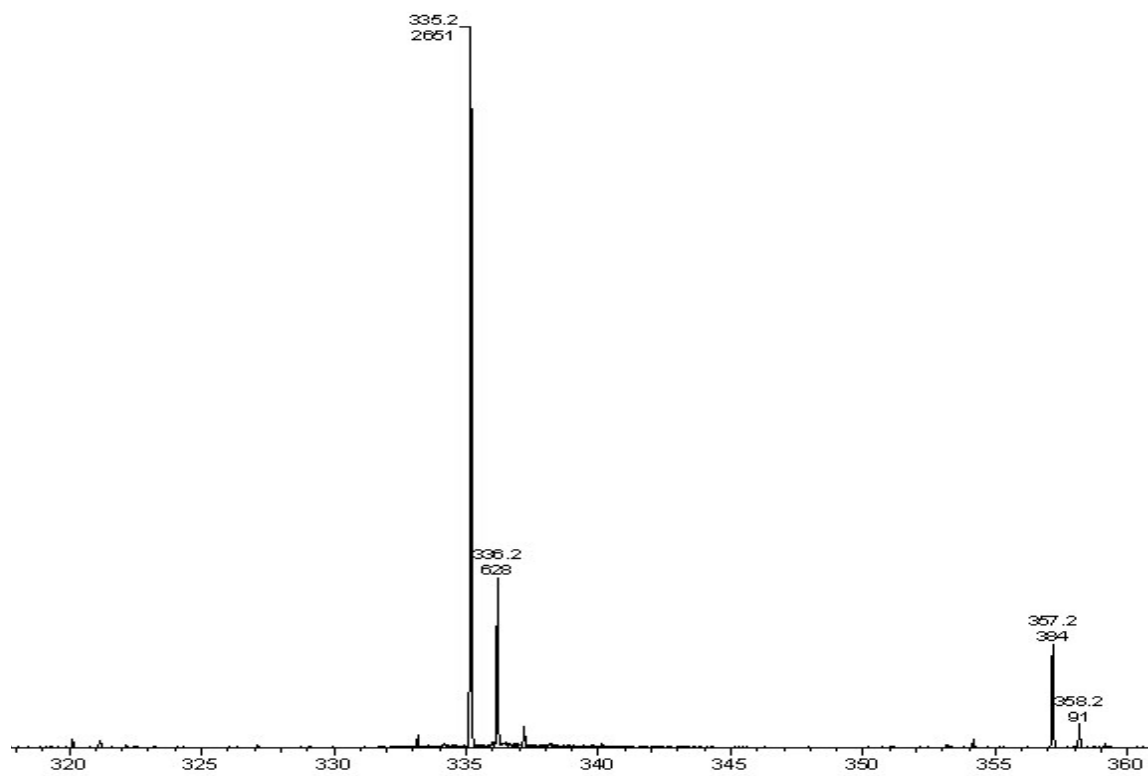


Figure S5. Mass spectrum of ligand L1.

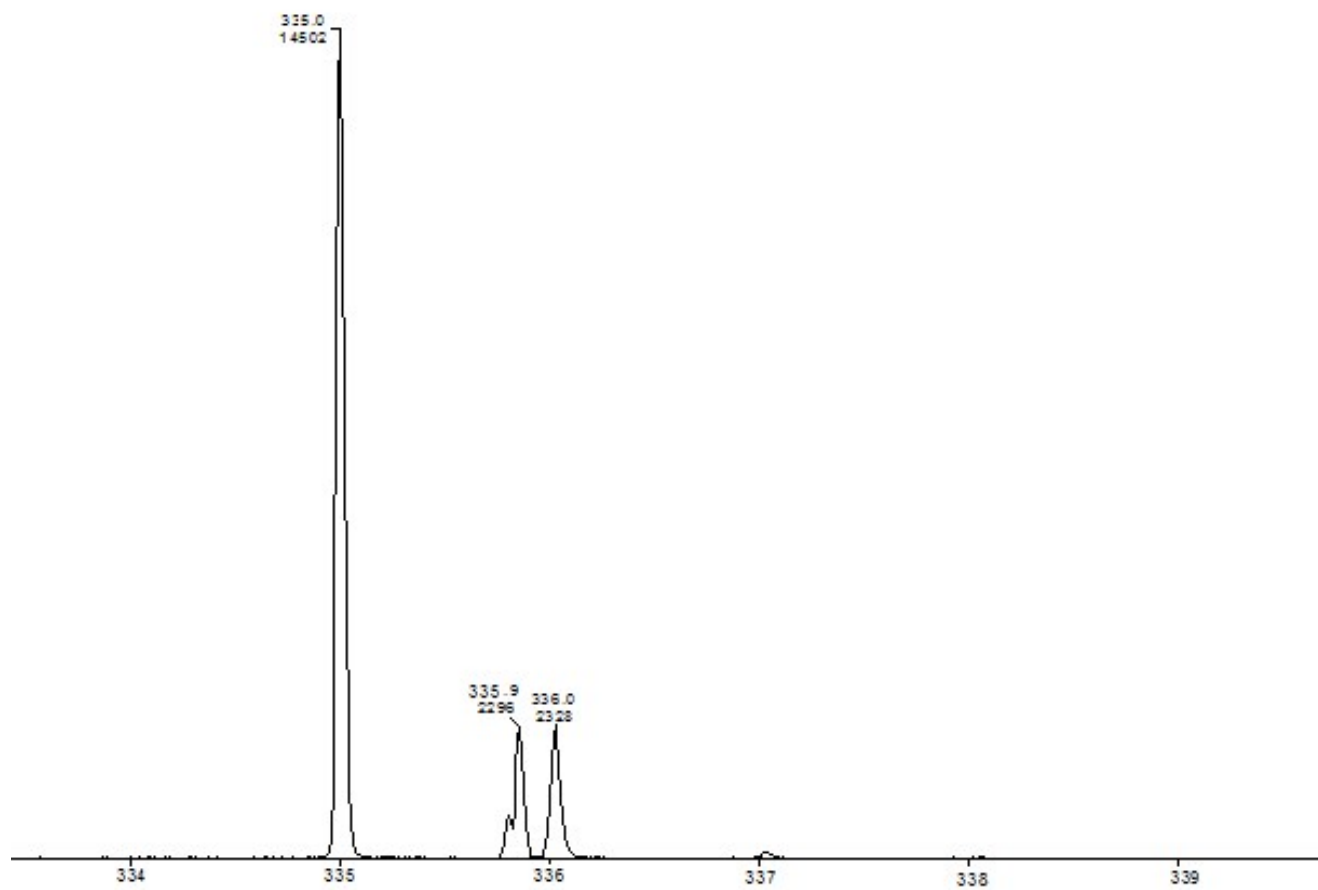


Figure S6. Mass spectrum of ligand L2.

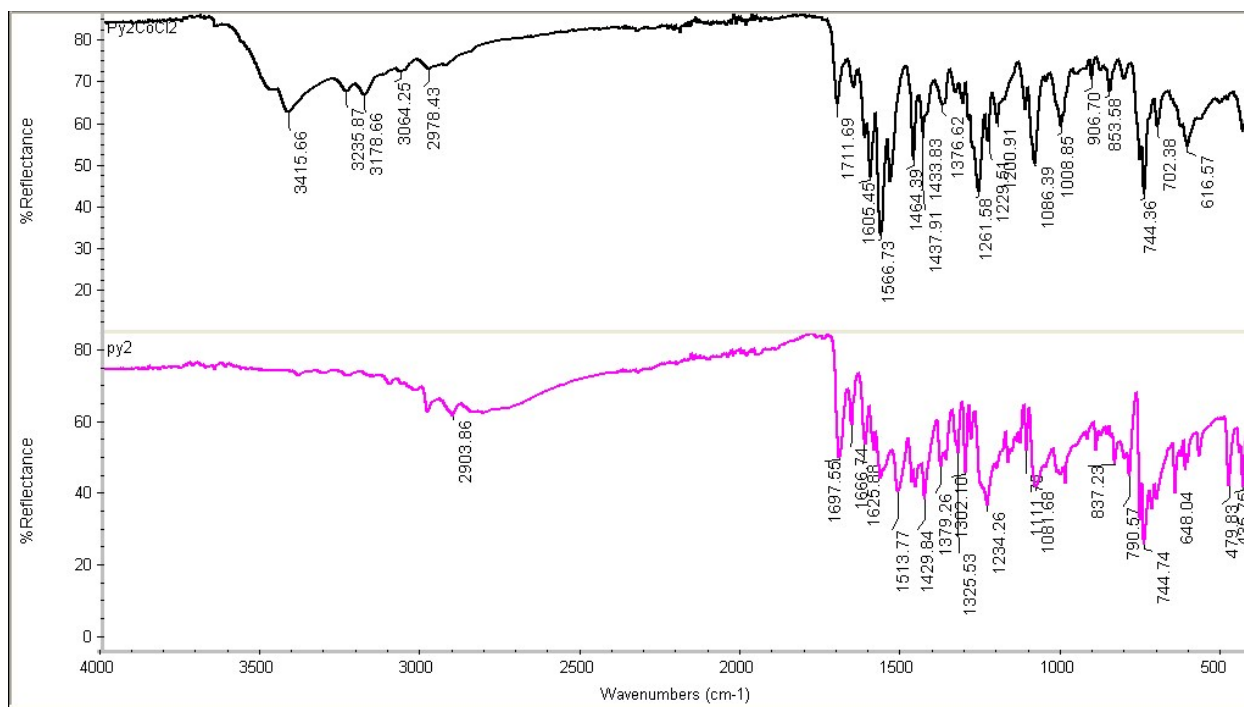


Figure S7. FTIR spectrum of ligand L1 (below) and its metal complex (top).

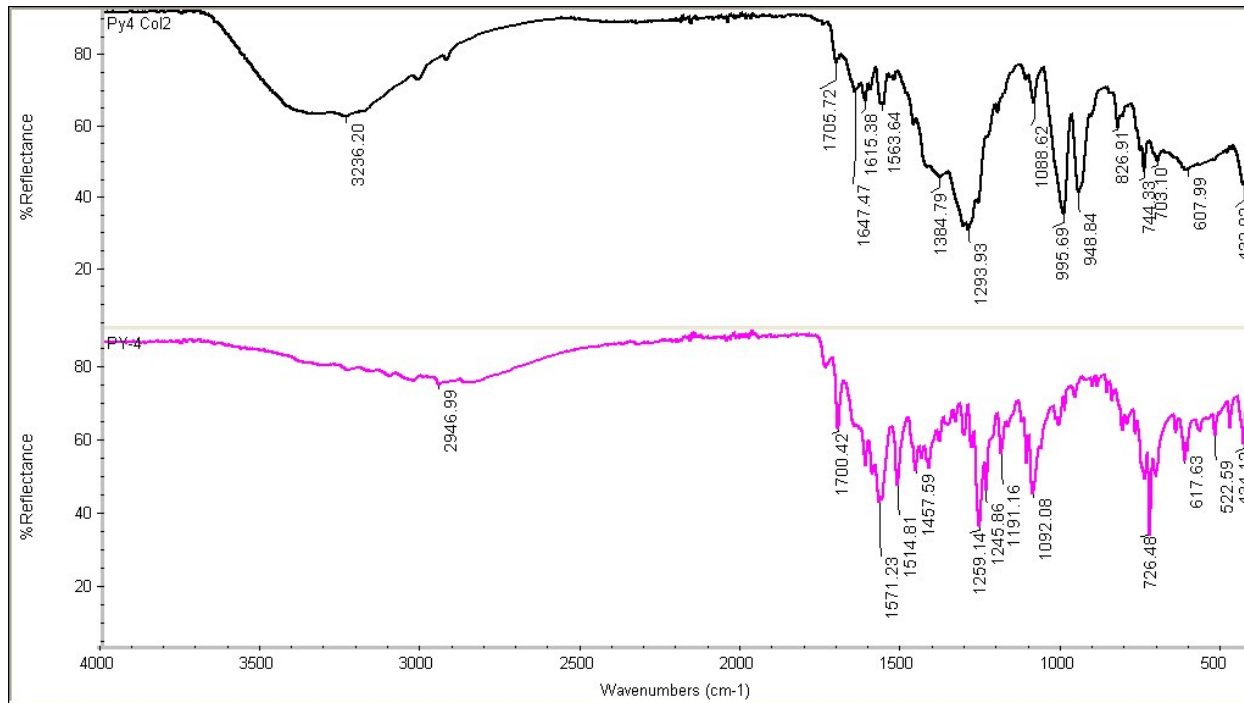


Figure S8. FTIR spectrum of ligand L2 (below) and its metal complex (top).

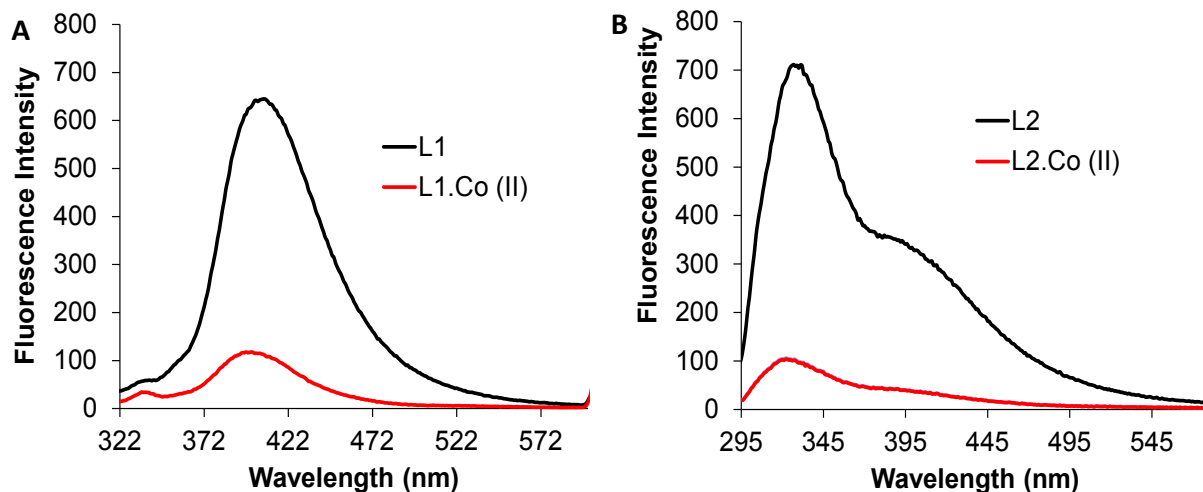


Figure S9. (A) Fluorescence spectra of ligand L1 in DMSO (10 μM) and its corresponding metal complex L1.Co (II). (B) Fluorescence spectra of ligand L2 in DMSO (10 μM) and its corresponding metal complex L2.Co (II).

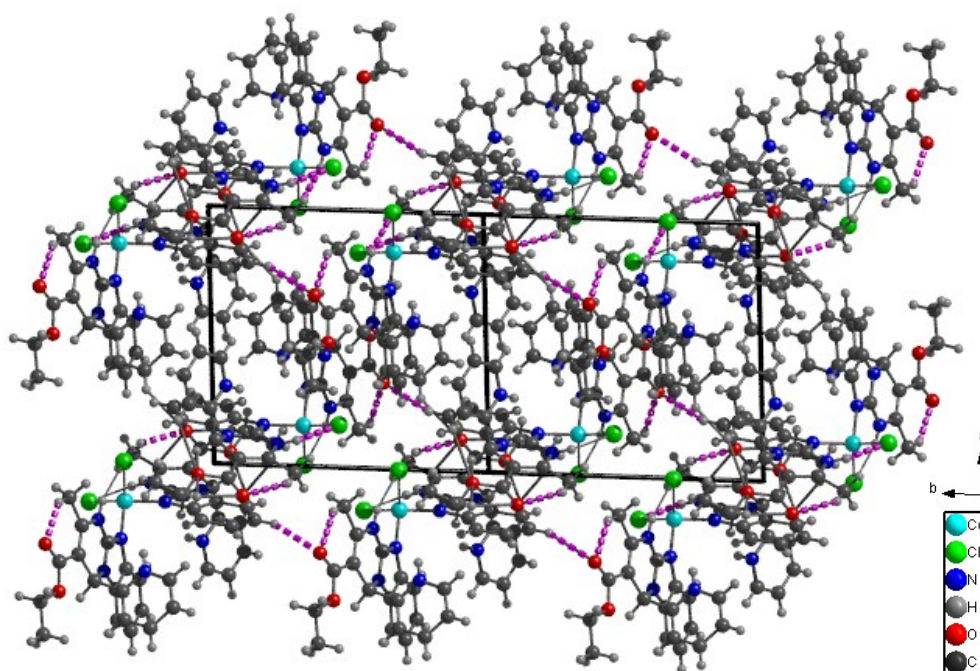


Figure S10. Packing diagram of complex L1.Co (II) shown down c axis (hydrogen bonding is shown by dotted pink lines).

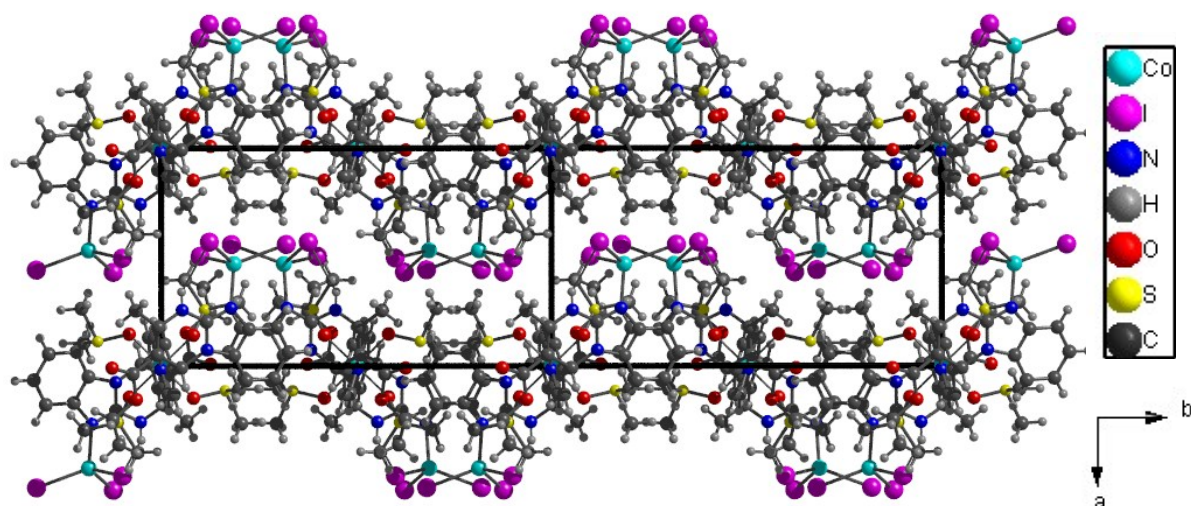


Figure S11. Packing diagram of complex L2.Co (II) shown down c axis.

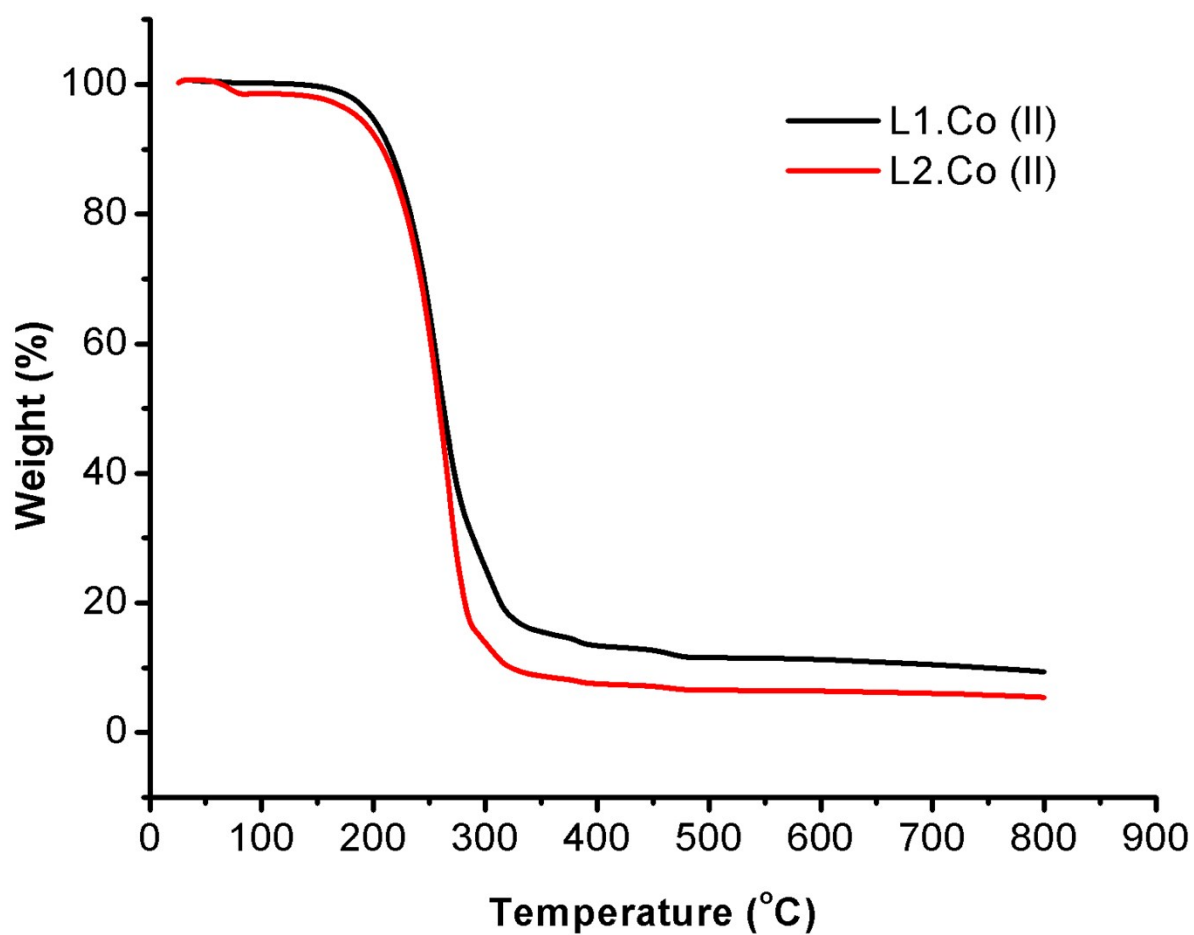


Figure S12. TGA graph of L1.Co (II) and L2.Co (II) complexes between the temperature range from 20 to 800 °C with the heating rate of 10 °C/minute.

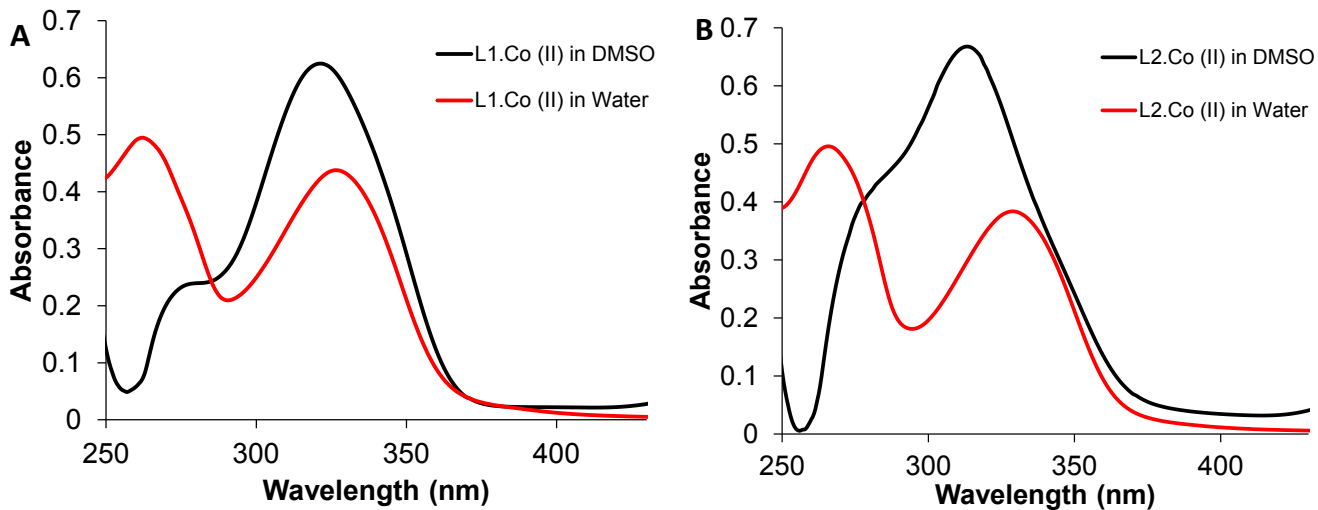


Figure S13. (A) UV-Vis absorption spectra of metal complex L1.Co (II) in DMSO and in aqueous medium. (B) UV-Vis absorption spectra of metal complex L2.Co (II) in DMSO and in aqueous medium.

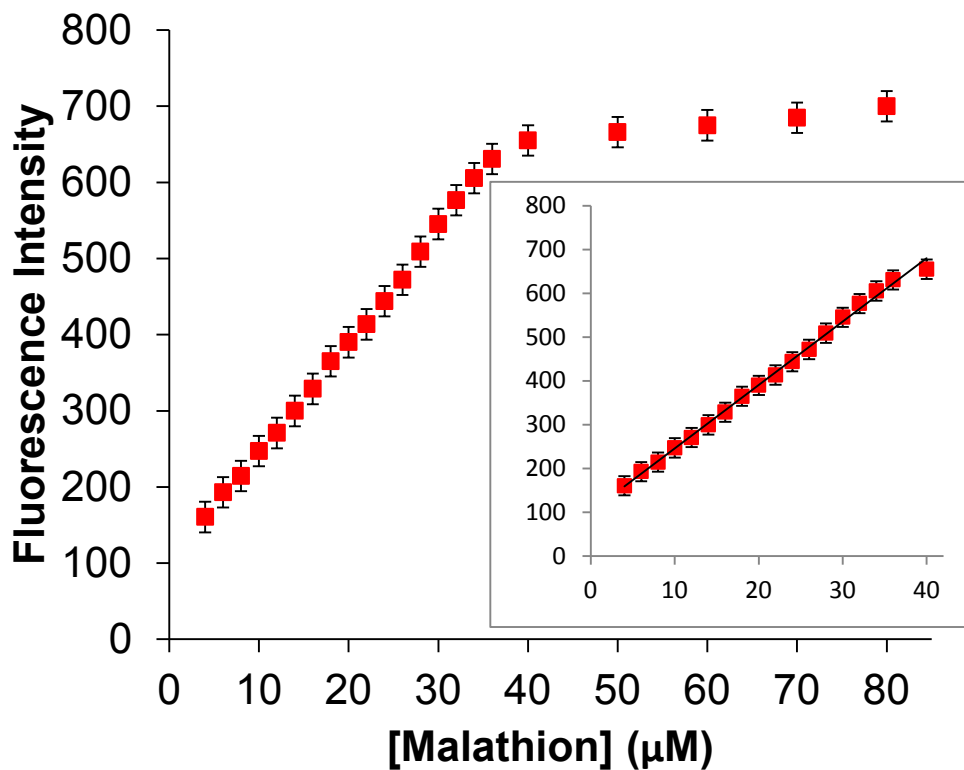


Figure S14. Non-linear regression graph between the emission intensity and concentration of Malathion added.

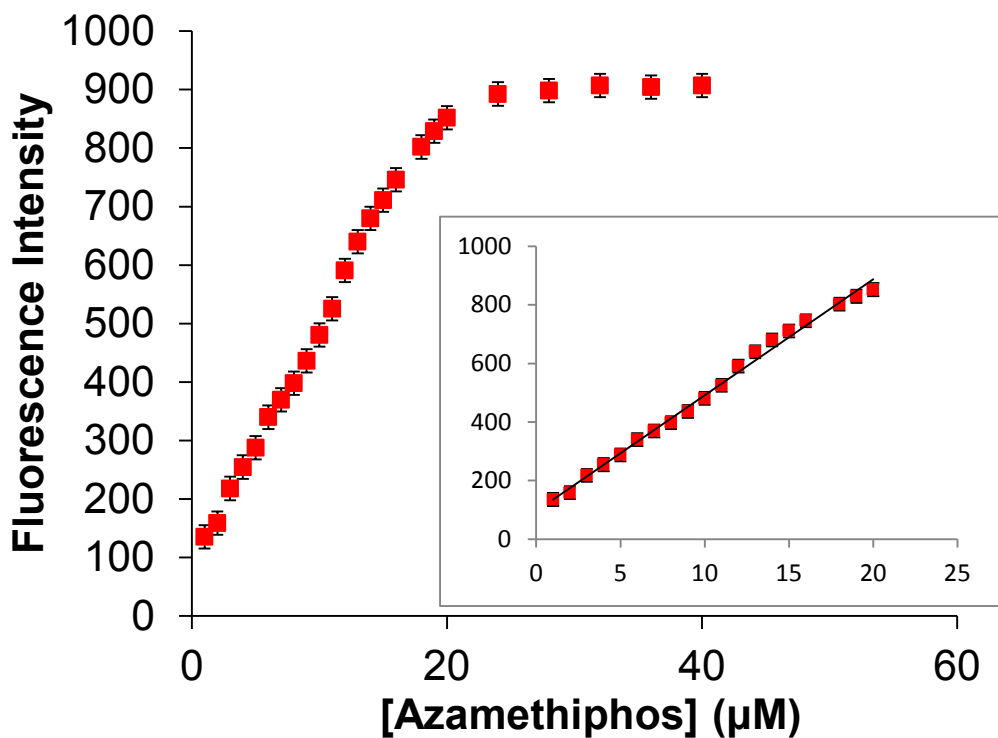


Figure S15. Non-linear regression graph between the emission intensity and concentration of Azamethiphos added.

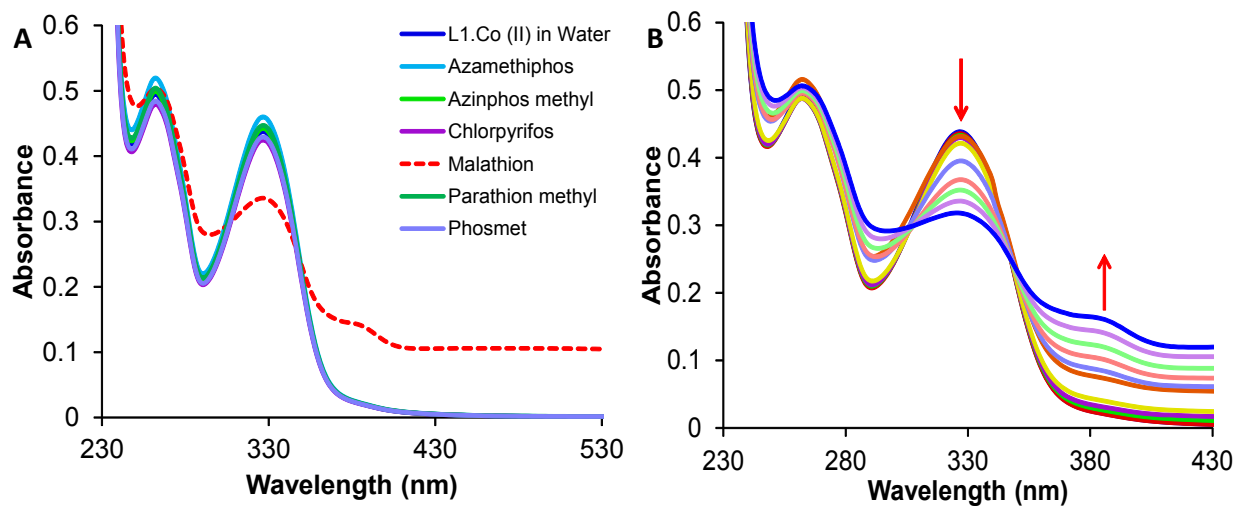


Figure S16. (A) UV- Vis absorption profile of metal complex L1.Co (II) in water upon addition of different organophosphates. (B) Titration of L1.Co (II) with increasing concentration of Malathion.

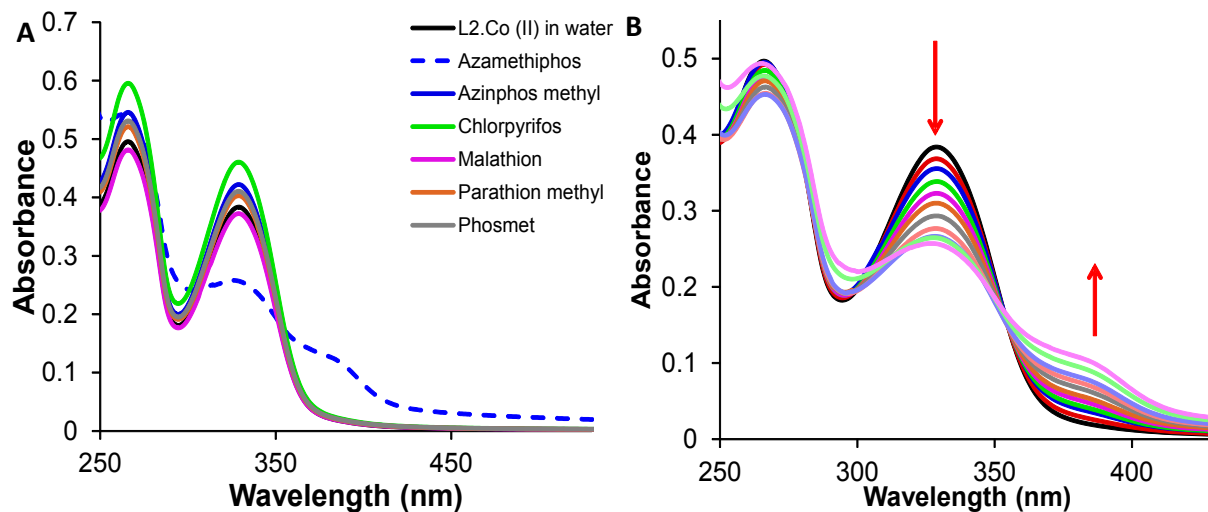


Figure S17. (A) UV-Vis absorption profile of metal complex L2.Co (II) in water upon addition of different organophosphates. (B) Titration of L2.Co (II) with increasing concentration of Azamethiphos.

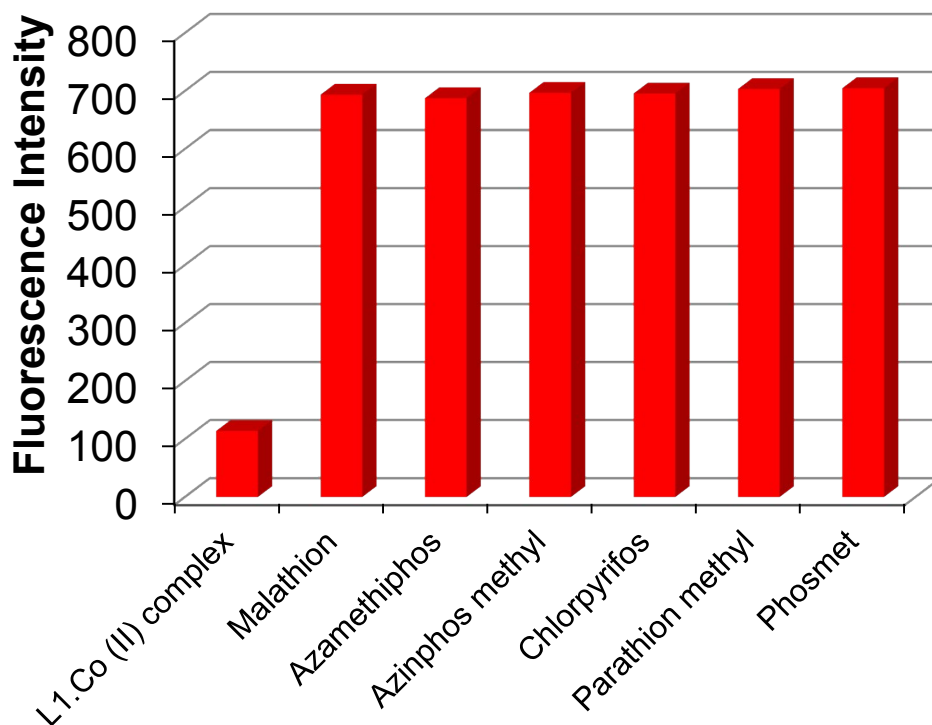


Figure S18. Competitive binding experiment of L1.Co (II) complex containing 45 μM of Malathion and 60 μM of other OPs under study.

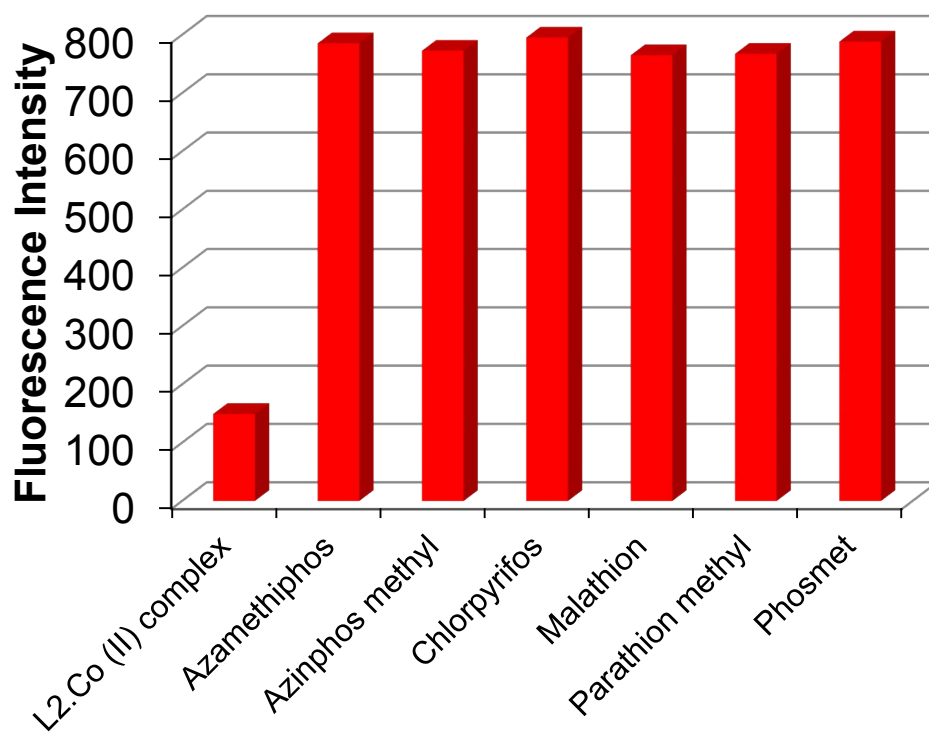


Figure S19. Competitive binding experiment of L2.Co (II) complex containing 15 μM of Azamethiphos and 60 μM of other OPs under study.

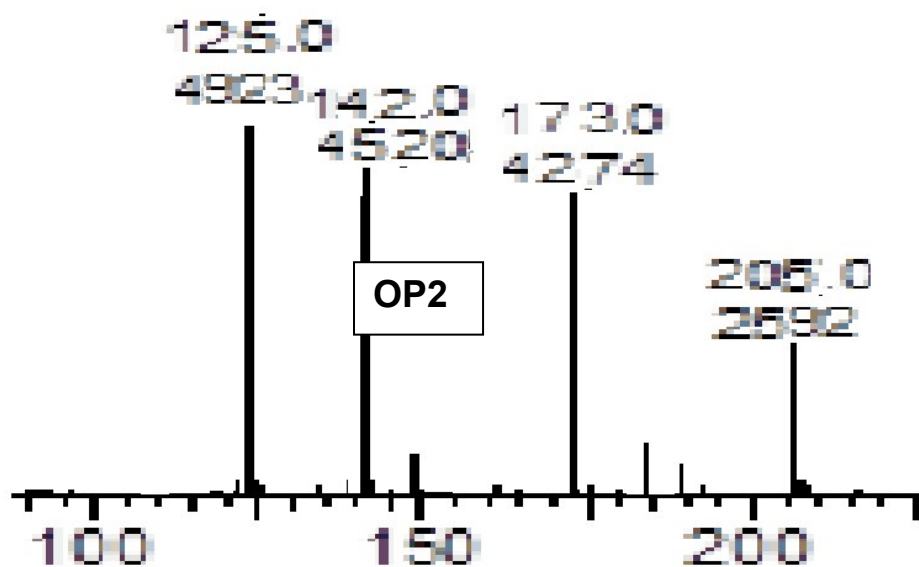


Figure S20. Mass spectra showing the degradation products of Malathion.

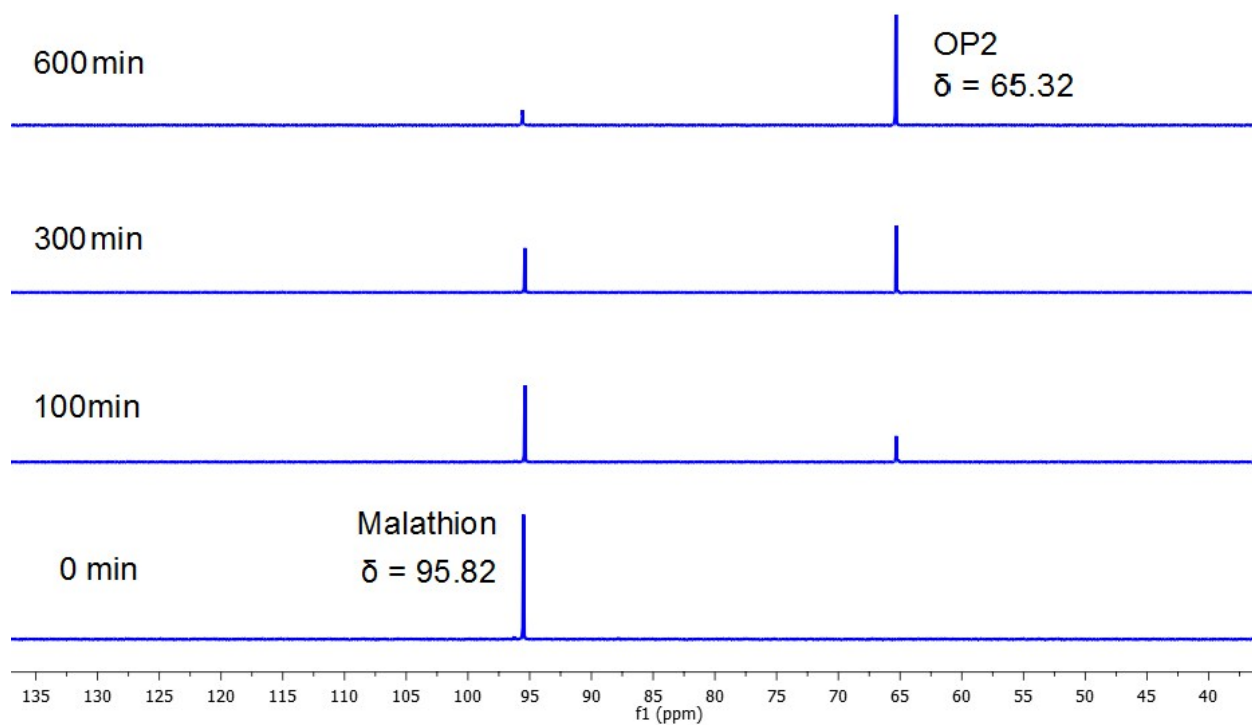


Figure S21. Change in ^{31}P -NMR signal of Malathion upon degradation with time.

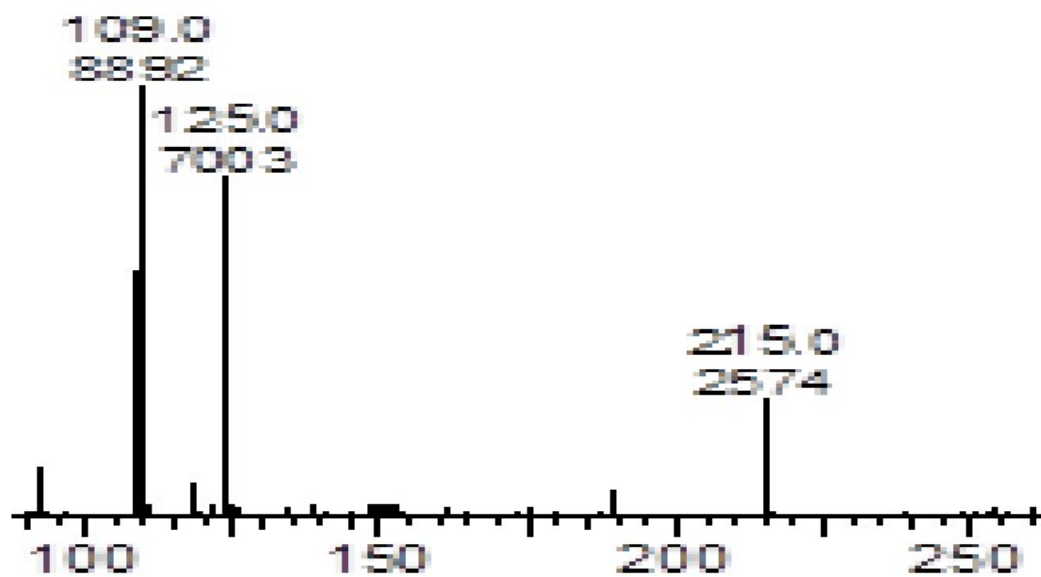


Figure S22. Mass spectra showing the degradation products of Azamethiphos.

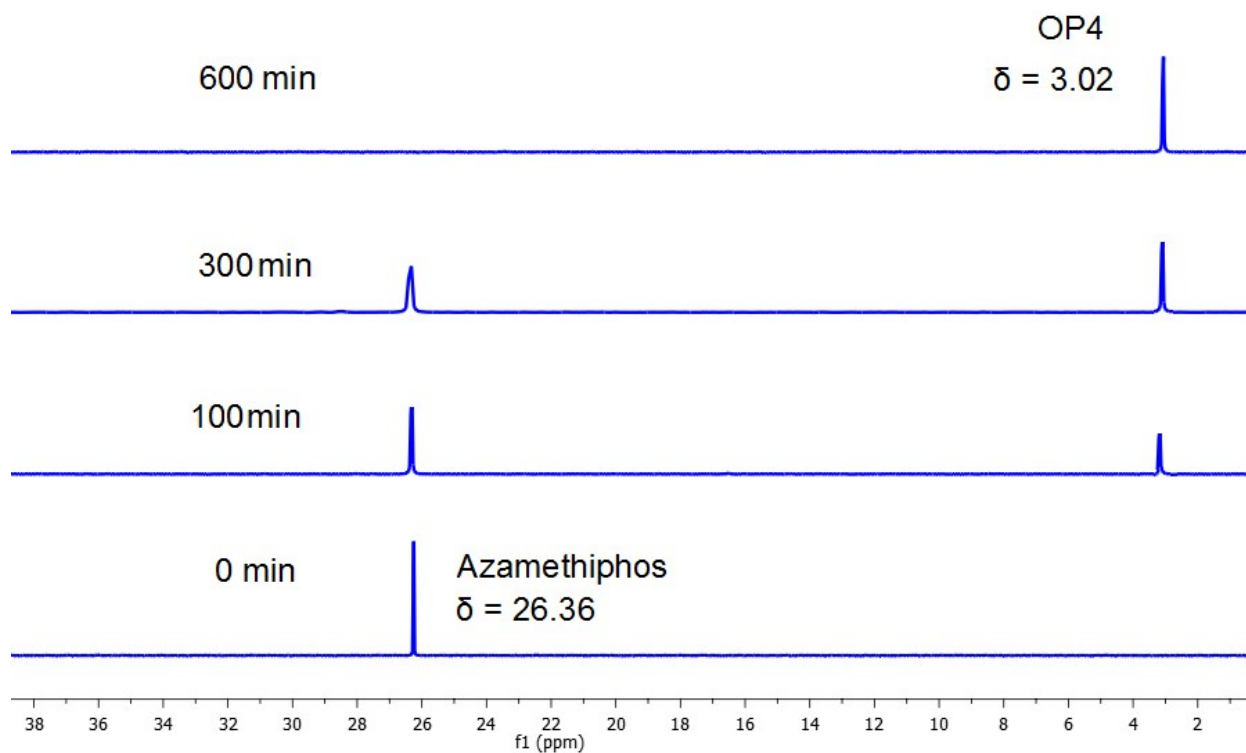


Figure S23. Change in ^{31}P -NMR signal of Azamethiphos upon degradation with time.

Hydrolysis experiments

1 mL of D_2O solution was buffered at pH 8.5 followed by addition of complex solution (1.5 μmol , DMSO, d_6). To this, malathion (or Azamethiphos) were added (25 μmol ,) and shaken vigorously before transferring to an NMR tube. ^{31}P NMR spectra were recorded for 6 hours and conversion was tracked by integrating the peaks associated with analyte versus the degradation product obtained. The solutions were buffered using CHES (pH 8.5)

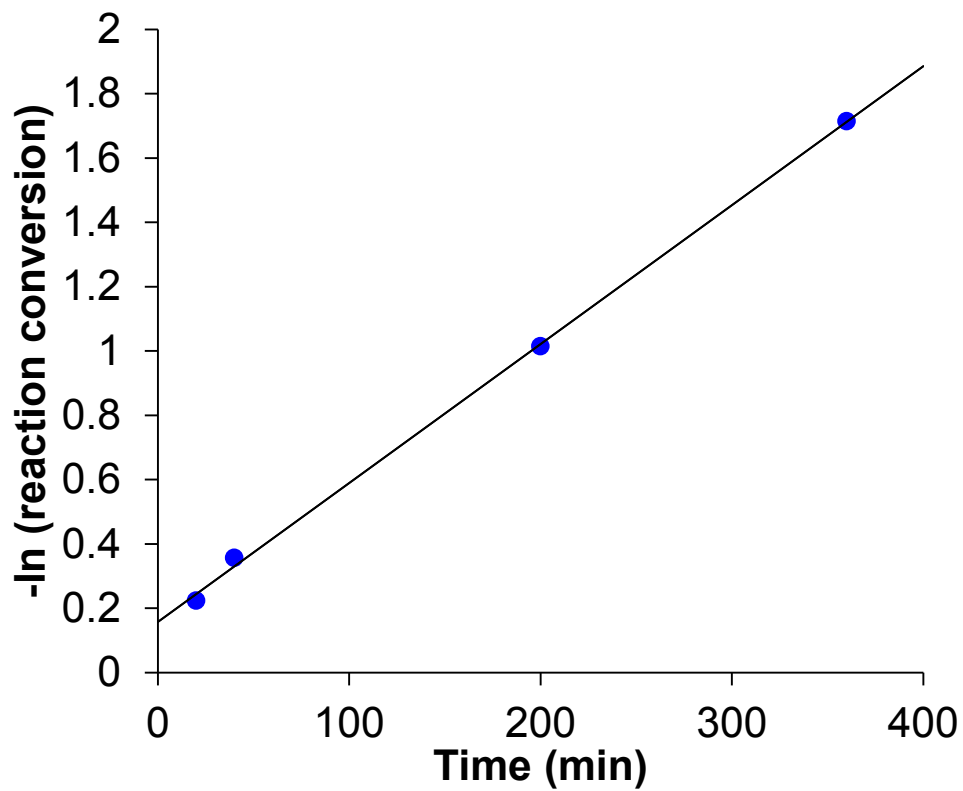


Figure S24. Kinetic plots showing the reaction of Malathion with L1.Co (II) in buffer solution. Initial half-life ($t_{1/2}$) was calculated by plotting \ln of the conversion versus time; the slope (k) is related to the half-life by $t_{1/2} = \ln 2/k$.

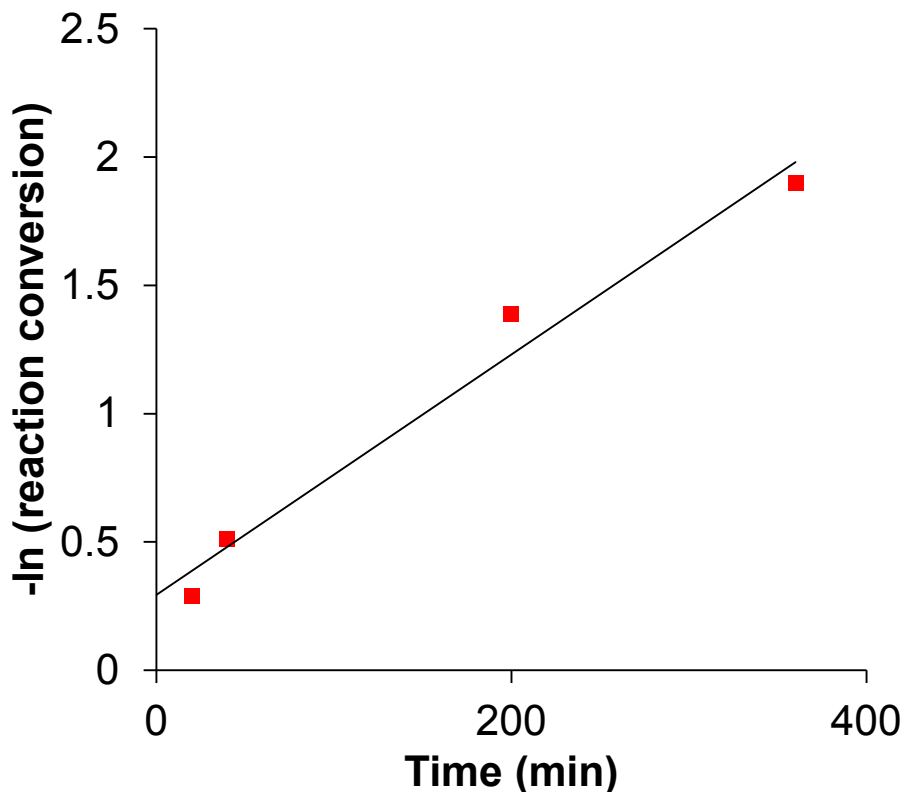


Figure S25. Kinetic plots showing the reaction of Azamethiphos with L2.Co (II) in buffer solution. Initial half-life ($t_{1/2}$) was calculated by plotting \ln of the conversion versus time; the slope (k) is related to the half-life by $t_{1/2} = \ln 2/k$.

Determination of limit of detection.

Linear regression graphs of titrations between the host and analyte were used to calculate standard deviation and slope of linear response. The limit of detection (LOD) of probes was determined using the following equation (IUPAC method)¹:

$$\text{LOD} = 3 \times \text{SD}/\text{Slope}$$

Where SD is the standard deviation of the blank solution and S is the slope of the calibration curve. The detection limits of both the probes were determined in a similar fashion.

1. G. L. Long, J. D. Winefordner, Limit of Detection: A Closer Look at the IUPAC Definition, *Anal. Chem.* 1983, 55, 712A–724A.

Table S1. Crystal data and refinement parameters of L1.Co (II).

Compound	L1.Co (II)
Empirical Formula	C ₃₈ H ₃₆ Cl ₂ CoN ₈ O ₄
M _w	798.58
Temperature [K]	293(2)
Crystal System	Triclinic
Space group	P-1
<i>a</i> / [Å]	11.4097(3)
<i>b</i> / [Å]	13.1465(3)
<i>c</i> / [Å]	13.9513(4)
α / [°]	66.5170(10)
β / [°]	83.3220(10)
γ [°]	84.4550(10)
V [Å ³]	1903.42(9)
Z	2
D _c [Mg m ⁻³]	1.393
μ / [mm ⁻¹]	0.642
Reflections collected	19434
Data / restraints / parameters	7452 / 0 / 483
Unique reflections, [R _{int}]	7452 [0.0354]
GOF = S _{all}	1.022
Final <i>R</i> indices	
R ₁ , wR ₂ [I>2 σ I]	0.0492, 0.1039
R ₁ , wR ₂ (all data)	0.0924, 0.1148
$\Delta\rho_{\max}/\Delta\rho_{\min}$ [Å ³]	0.314/ -0.416

Table S2. Selected bond lengths and angles (Å,°) for complex L1.Co (II).

Bond lengths(Å)					
Co(1)-N(1)	1.998(2)	Co(1)-Cl(1)	2.2614(9)	N(2)-C(1)	1.341(3)
Co(1)-N(5)	2.002(2)	N(1)-C(1)	1.325(3)	N(2)-C(7)	1.404(3)
Co(1)-Cl(2)	2.2459(8)	N(1)-C(2)	1.412(3)	N(2)-C(8)	1.463(3)
Bond angles(°)					
N(1)-Co(1)-N(5)	108.43(9)	N(1)-Co(1)-Cl(1)	109.19(7)	C(1)-N(1)-C(2)	104.2(2)
N(1)-Co(1)-Cl(2)	106.91(7)	N(5)-Co(1)-Cl(1)	105.42(7)	C(1)-N(1)-Co(1)	128.35(18)
N(5)-Co(1)-Cl(2)	109.21(7)	Cl(2)-Co(1)-Cl(1)	117.43(4)	C(2)-N(1)-Co(1)	126.42(17)

Table S3. Hydrogen bonding parameters (Å, °) of L1.Co (II).

D-H...A	D...A/ Å	H...A/ Å	D-H...A/°
N3-H3A...Cl2	3.240(3)	2.448(1)	153.4(2)
N7-H7A...Cl1	3.165(3)	2.370(1)	154.0(2)
C11-H11A...O1	2.836(5)	2.093(3)	133.1(2)
C14-H14A...O3ⁱ	3.237(5)	2.518(3)	134.3(3)
C24-H24A...O1ⁱⁱ	3.438(4)	2.558(2)	158.1(3)
C30-H30A...O3	2.845(6)	2.128(4)	130.3(3)
C32-H32A...O4	3.158(5)	2.540(3)	124.2(3)
C38-H38B...O3 (7)	3.564(8)	2.719(3)	147.2(4)

Equivalent positions: (i) - x-1,+y,+z+1, (ii) x,+y-1,+z,

Table S4. Crystal data and refinement parameters of L2.Co (II).

Compound	L2.Co (II)
Empirical Formula	C ₄₆ H ₆₀ Co ₃ I ₆ N ₈ O ₈ S ₄
M _w	1919.45
Temperature [K]	293(2)
Crystal System	Monoclinic
Space group	P2 ₁ /c
<i>a</i> / [Å]	10.2940(3)
<i>b</i> / [Å]	18.0946(5)
<i>c</i> / [Å]	18.0830(5)
α / [°]	90
β / [°]	100.9810(10)
γ / [°]	90
V [Å ³]	3306.57(16)
Z	2
D _c [Mg m ⁻³]	1.928
μ / [mm ⁻¹]	3.721
Reflections collected	35606
Data / restraints / parameters	6489 / 0 / 359
Unique reflections, [R _{int}]	6489 [0.0376]
GOF = S _{all}	1.016
Final <i>R</i> indices	
R ₁ , wR ₂ [I > 2σI]	0.0389, 0.0930
R ₁ , wR ₂ (all data)	0.0510, 0.0977
$\Delta\rho_{\max}/\Delta\rho_{\min}$ [Å ³]	1.232/-1.245

Table S5. Selected bond lengths and angles (Å,°) for complex L2.Co (II).

Bond lengths(Å)					
Co(1)-N(1)	2.075(4)	Co(2)-O(4)	2.095(3)	S(1)-C(21)	1.781(7)
Co(1)-I(1)	2.563(5)	Co(2)-O(3)	2.104(3)	N(1)-C(1)	1.318(5)
Co(1)-I(2)	2.594(5)	Co(2)-N(4)	2.149(3)	C(2)-C(3)	1.385(6)
Co(1)-I(3)	2.6254(6)	O(3)-S(1)	1.517(3)		
Bond angles(°)					
N(1)-Co(1)-I(1)	101.81(16)	I(1)-Co(1)-I(3)	108.48(17)	O(4)-Co(2)-N(4)	96.33(13)
N(1)-Co(1)-I(2)	114.41(14)	I(2)-Co(1)-I(3)	107.98(11)	O(3)-Co(2)-N(4)	89.29(12)
I(1)-Co(1)-I(2)	119.03(17)	O(4)-Co(2)-O(3)	90.54(13)	O(3)-S(1)-C(21)	103.8(3)
N(1)-Co(1)-I(3)	104.01(10)	O(3)-Co(2)-O(3)#1	180.00(12)	O(3)-S(1)-C(20)	105.4(3)

Table S6. Hydrogen bonding parameters (Å, °) of L2.Co (II)

D-H...A	D...A/ Å	H...A/ Å	D-H...A/°
C11-H11A...O1	2.882(7)	2.141(5)	133.0(4)
C20-H20B...O1 ⁱ	3.436(7)	2.560(4)	151.7(4)

Equivalent positions: (i) -x+2,+y+1/2,-z+1/2

Reference:

1. G. M. Sheldrick, Acta Crystallogr. A, 2008, 64, 112–122.
2. A. Altomare, M. C. Burla, M. Camalli, G. L. Cascarano, C. Giacovazzo, A. Guagliardi, A. G. Moliterni, G. Polidori, R. Spagna, J. Appl. Crystallogr. 1999, 32, 115-119.
3. L.J. Farrugia, J. Appl. Crystallogr. 1999, 32, 837.
4. M. Nardelli, J. Appl. Crystallogr. 1995, 28, 659.
5. W. T. Pennington, DIAMOND - Visual Crystal Structure Information System, J. Appl. Cryst. 1999, 32, 1028.